AN EXPERIMENTAL STUDY ON OUT-OF-PLANE DEFORMATIONS OF RECTANGULAR STRUCTURAL WALLS SUBJECT TO IN-PLANE LOADING

F. Dashti[(1)], R. P. Dhakal[(2)], S. Pampanin[(3)]

[(1)] *PhD Candidate, Dept. of Civil and Natural Resources Engineering, University of Canterbury, farhad.dashti@pg.canterbury.ac.nz*
[(2)] *Professor, Dept. of Civil and Natural Resources Engineering, University of Canterbury, rajesh.dhakal@canterbury.ac.nz*
[(2)] *Professor, Dept. of Civil and Natural Resources Engineering, University of Canterbury, stefano.pampanin@canterbury.ac.nz*

Abstract

Out-of-plane instability is identified as one of the failure modes of rectangular RC walls. This mode of failure was previously observed in experimental studies of rectangular walls, and has attracted more attention following the observed damage of several walls in the recent earthquakes in Chile and Christchurch.

In this study, out-of-plane instability of slender rectangular walls subject to in-plane loading is investigated by testing three rectangular wall specimens subject to cyclic quasi-static loading. The specimens were half-scale, representing the first story of four story prototype walls designed according to NZS3101:2006, with different thicknesses and lengths to investigate the effects of these parameters on the onset and extent of out-of-plane displacement. The experimental results are herein presented with focus on the significant stages of wall response observed during the test and the effects of the above-mentioned parameters on the sequence of these stages.

Keywords: Structural wall, Out-of-plane deformation, Experimental study, Wall thickness, Wall length

1. Introduction

According to the observations of the recent earthquakes in Chile and New Zealand, the lateral instability of a large portion of a wall section (also referred to as out-of-plane buckling/instability) was one of the failure patterns that raised concerns about the performance of buildings designed using modern codes [1]. Prior to the Chile earthquake, this failure mechanism had only been primarily observed in laboratory tests [2, 3, 4]. Out-of-plane buckling/instability refers to the (local) buckling of a portion of a wall section out-of-plane, as a result of inelastic flexural response during an earthquake. The out-of-plane buckling is typically limited to an end region of the wall where vertical tension and compression strains from in-plane cyclic flexure are greatest [5].

Paulay and Priestley [6] made recommendations for the prediction of the onset of out-of-plane instability based on the observed response in tests of rectangular structural walls and theoretical considerations of fundamental structural behaviour. Because of very limited available experimental evidences, engineering judgement was relied on extensively. It was concluded that such inelastic buckling mechanism is more affected by wall length than by unsupported height and the major source of the instability was postulated to be the previously experienced tensile strain than maximum compression strain.

In order to address this mode of failure, researchers have usually tested columns representing boundary zones of rectangular walls. Chai and Elayer [7] studied the out-of-plane instability of ductile RC walls by idealizing the end-region of the wall as an axially loaded RC column, as shown in Fig. 1, and conducted an experimental study to examine the out-of-plane instability of several RC columns that were designed to represent the end-regions of a ductile planar RC wall under large amplitude reversed cyclic tension and compression.

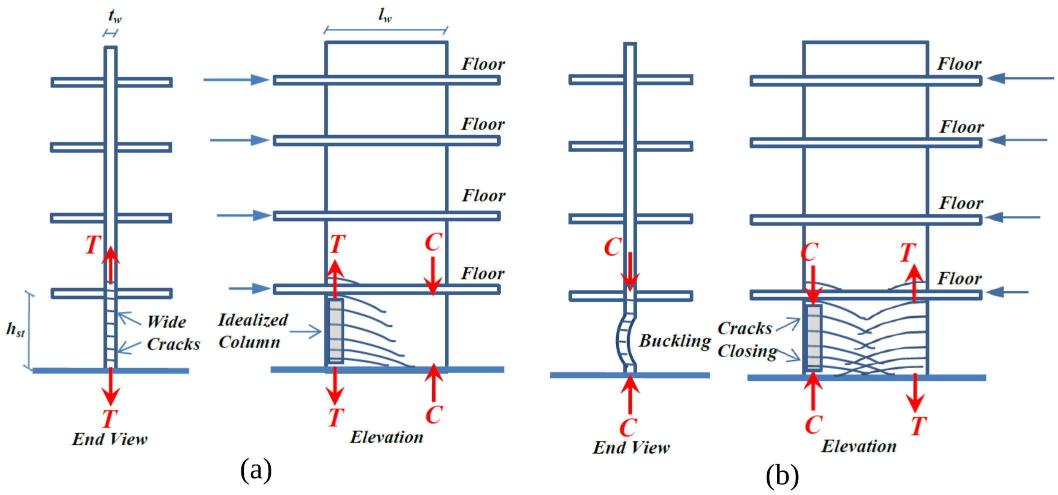

Fig. 1 Idealization of reinforced concrete wall in end regions: (a) opening of cracks under tension cycle; and (b) closing of cracks under compression cycle [7]

Rosso, et al. [8] investigated the out-of-plane failure mode of walls by analyzing the response of two singly reinforced T-shaped walls tested under cyclic loading. The specimens were identical but were subjected to two different loading patterns, i.e. in-plane and bi-directional.

In this study the effects of the parameters known to be influential on out-of-plane instability of rectangular structural walls are investigated by analyzing the response of three wall specimens designed according to the current New Zealand concrete standard [9] and tested under in-plane cyclic loading.

2. Test Matrix

In order to identify the parameters affecting the initiation and development of out-of-plane deformations in rectangular walls, a parametric study was conducted using a numerical model that had been verified for its capability to simulate different failure modes of this type of structural walls [10]. In addition to the parametric study, a detailed investigation of the wall response at the material level and at different stages of development of out-of-plane deformations was carried out and the formation of out-of-plane deformation in the numerical model was scrutinized with reference to the postulations and experimental observations of other researchers [11]. Wall thickness, length and axial load ratio were identified as the main parameters controlling this mode of deformation in rectangular walls. A four-specimen test matrix was designed (Table 1) to investigate these parameters. However, due to the structural laboratory decanting and refurbishment process, the effect of axial load could not be investigated and the last specimen was not tested.

Table 1. Test specimens

Parameter	Specimen	Length, l_w, mm	Thickness, t_w, mm	Length of boundary elements, mm	Axial load, kN	Longitudinal reinforcement ratio	
						Boundary region	Web
Benchmark	RWB	2000	125	350	438	0.026	0.0059
Thickness	RWT	2000	135	350	438	0.024	0.0055
Length	RWL	1600	125	300	438	0.043	0.012
Axial load	RWA	2000	125	350	657	0.026	0.0059

Specimen RWB is considered the benchmark specimen and differs from each other specimens in just one of the above-mentioned parameters. Specimen RWT differs from Specimen RWB in its thickness. This specimen was slightly larger in thickness. Specimen RWL was shorter when compared to Specimen RWB, and consequently had larger longitudinal reinforcement ratio in the boundary region to compensate for the reduction of the moment capacity coming from the reduction of the flexural lever arm of the section. Specimen RWA was exactly identical to Specimen RWB and was supposed to be subjected to a higher axial load ratio. The specimens were all designed according to the latest version of the New Zealand Concrete Standard [9]. Fig. 2 displays the geometry and reinforcement configuration of the specimens.

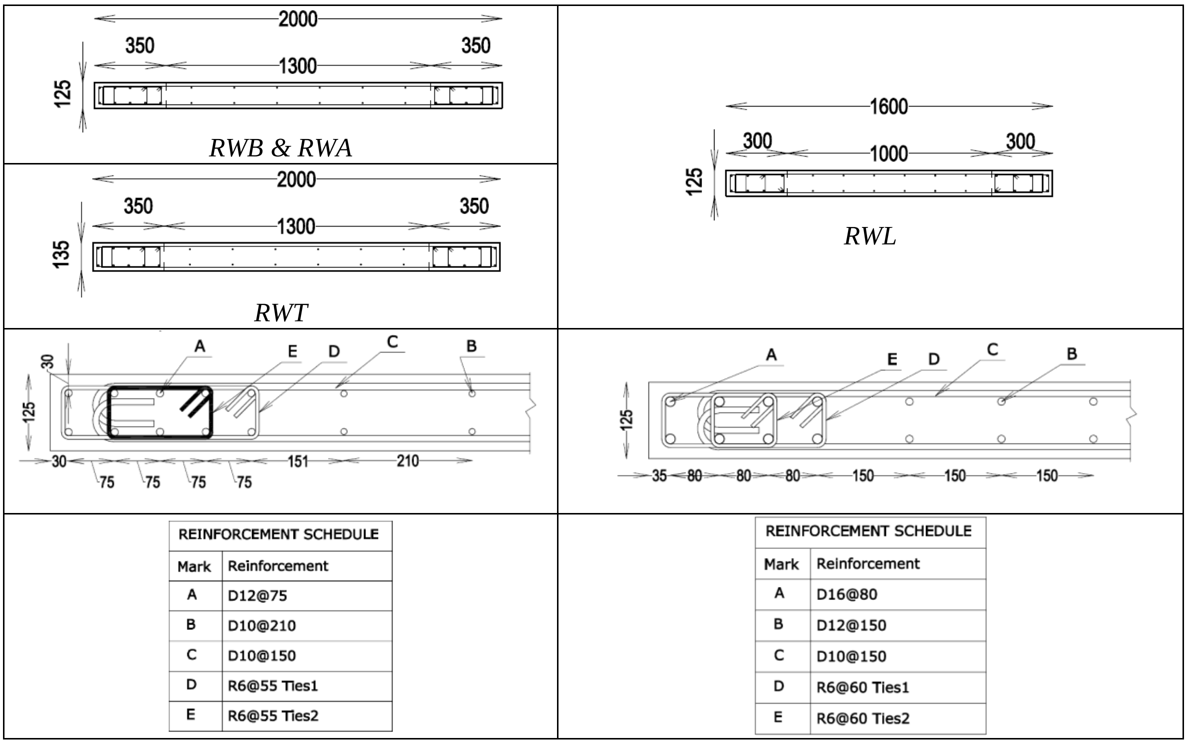

Fig. 2 Geometry and reinforcement configuration of the specimens

The test specimens were half-scale models of the prototype walls and represented the first story of a four-storey high wall. Fig. 3 displays the dimensions of the prototype wall and the specimen as well as the loadings applied on the specimen. The test setup was thus designed to apply the lateral load as well as the bending moment coming from the upper stories. Fig. 4 displays the configuration of horizontal and vertical actuators producing this loading pattern. As movements of the horizontal and vertical actuators were interdependent, the control program was designed to balance the actuators at each step through an iterative approach so that they comply with the above mentioned loading conditions and satisfy the design shear-span ratio. The out-of-plane deformation of the specimen was restricted at loading level using two roller supports at each side of the loading beam.

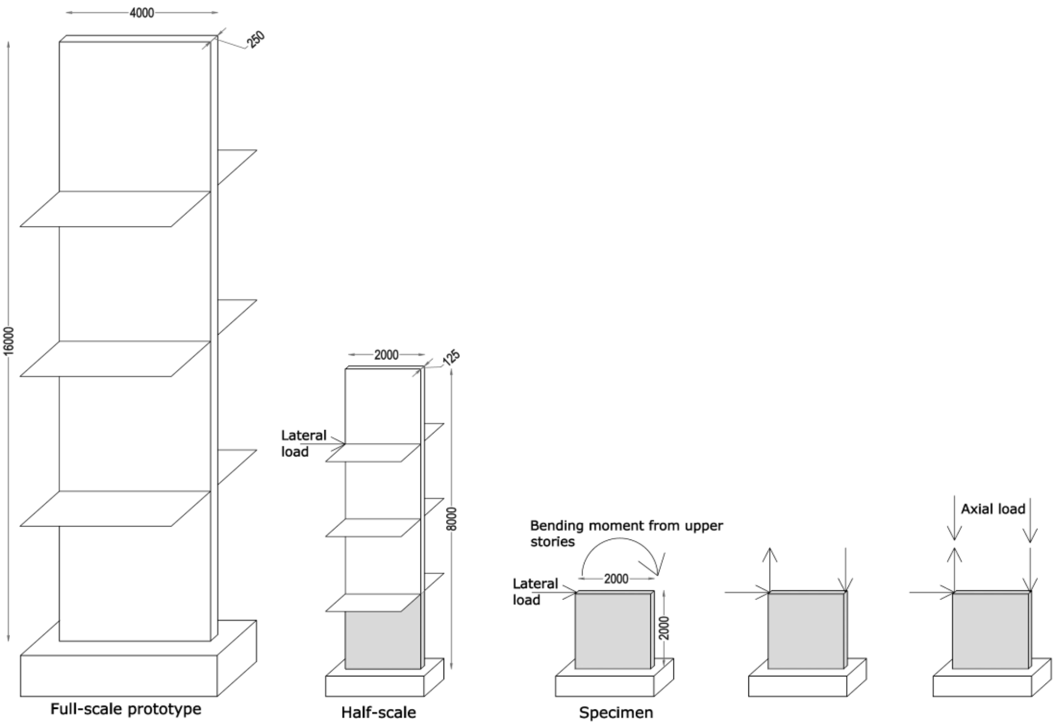

Fig. 3 Specimen scaling and loading pattern

The specimens were subjected to a quasi-static cyclic loading regime with three cycles at each drift level. Fig. 5 displays the displacement history applied using the horizontal actuator (Fig. 4). Specimens RWB, RWT and RWL were subjected to axial load ratio, ν=N/(f'cAc), of 0.05, and Specimen RWA was supposed to be subjected to an axial load ratio of 0.075. The loading applied by the vertical actuators consisted of the axial load and the bending moment corresponding to every increment of lateral displacement.

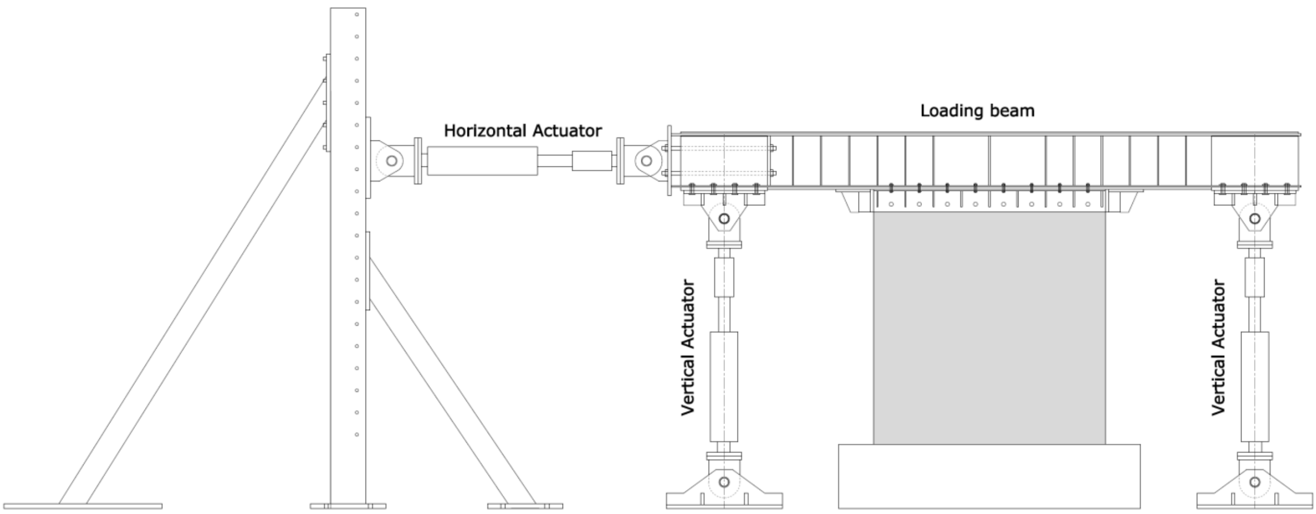

Fig. 4 Test setup

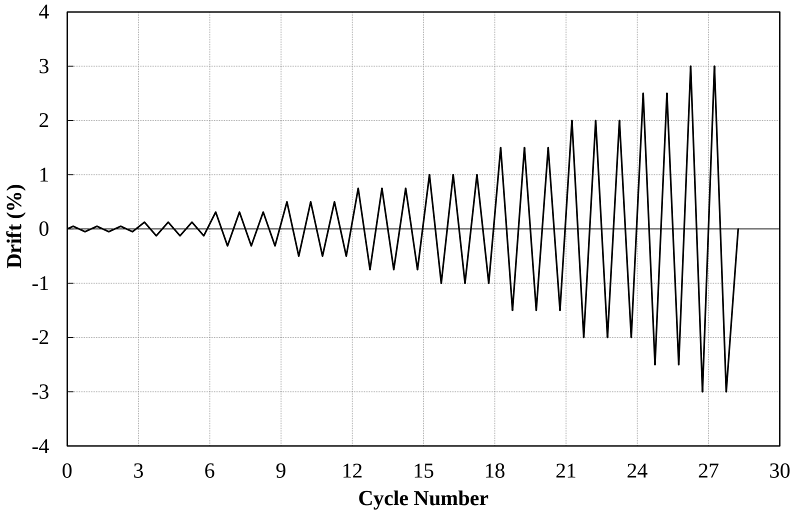

Fig. 5 Applied displacement history

3. Instrumentation

The instrumentation of the specimens was done to capture as much information as possible regarding initiation and development of out-of-plane deformations. For this purpose, 36 linear potentiometers were attached to the boundary zones at two faces of the wall to measure the vertical displacements of the wall boundary regions at different positions along the wall height. This information could be used to capture the variation of vertical displacements along the wall thickness and identify the loading stage corresponding to initiation of out-of-plane displacements. Fig. 6a and Fig. 6b indicate these linear potentiometers at north and south faces of the specimen, respectively. As can be seen in Fig. 6a, in addition to the potentiometers attached to the boundary regions, three potentiometers were used along the wall panel and at the base, to capture the variation of vertical displacements along 300mm distance from the base, and help to analytically derive the nonlinear strain profile along the wall length and identify the neutral axis position at different stages of loading. Also, the 250x250mm grid shown in Fig. 6a was used to visualize the crack and deformation patterns at different positions of the wall. The shear deformation of the wall panel was measured using the diagonal potentiometers shown in Fig. 6b. Fig. 6c displays one of the out-of-plane supports provided for the loading beam as well as the load cell attached to the roller to measure the variations of the out-of-plane load at different stages of loading.

Reinforcement strain at different stages of loading, unloading and reloading has been identified as one of the main parameters controlling out-of-plane deformations of rectangular walls. In order to investigate the effect of this parameter, in addition to 70 strain gauges attached to the reinforcement along the half-height of the wall, couplers were welded to the longitudinal reinforcement at each extreme end (Fig. 6a and Fig. 6b) to capture the average reinforcement strain along the distance between two couplers (400-550mm). Fig. 6c displays a typical string potentiometer used for measuring the out-of-plane deformations of the specimens. Such potentiometers were attached to both boundary regions and along half height of the wall.

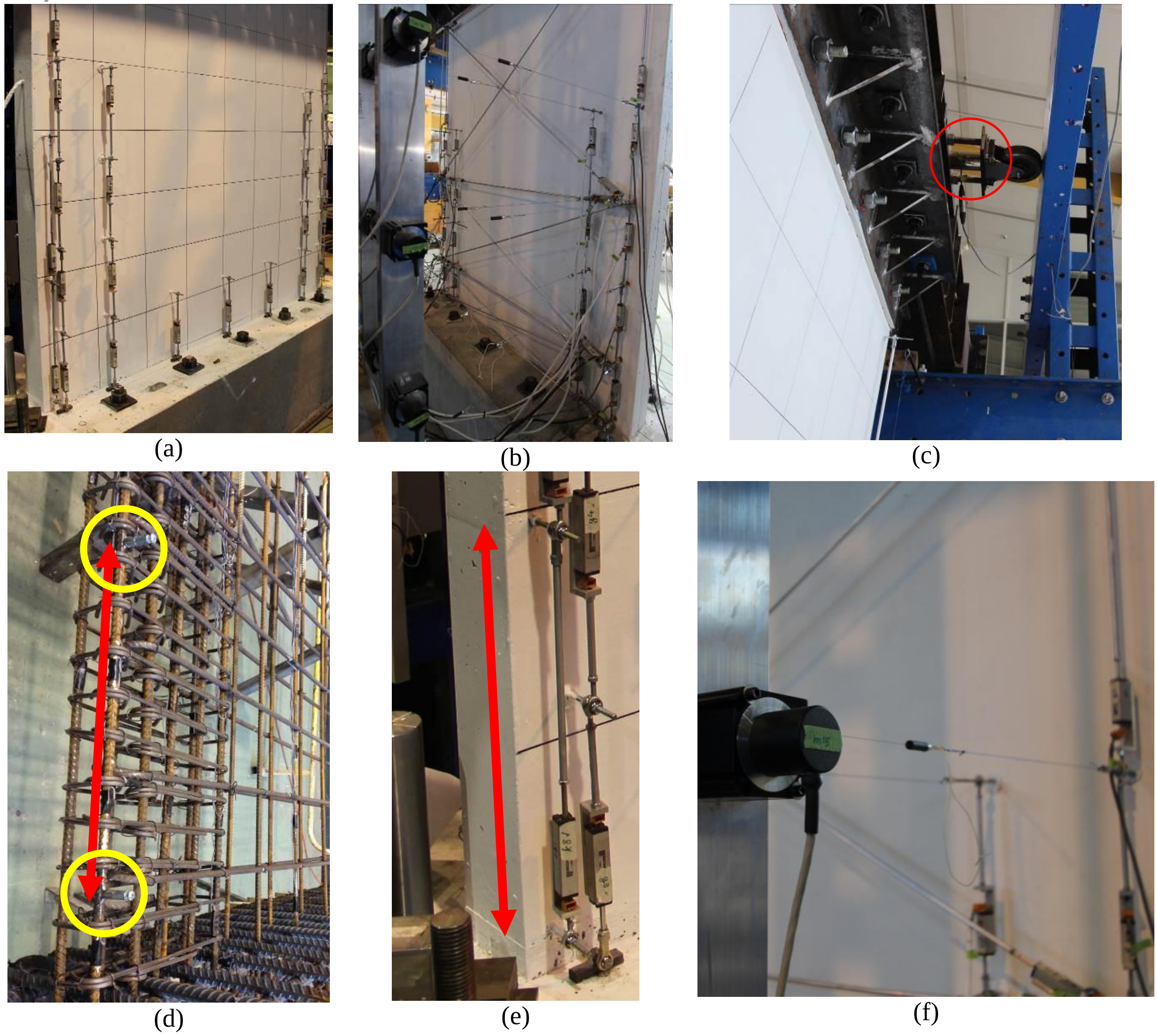

Fig. 6 Instrumentation: (a) linear potentiometers-north face; (b) linear potentiometers-south face; (c) load cell attached to out-of-plane support of the beam(d) strain gauges and welded couplers; (e) linear potentiometer attached to the couplers for measuring the average reinforcement strain; (f) string potentiometer for measuring out-of-plane displacements

4. Response of the specimens

Since Specimen RWB was the benchmark specimen, its response is described in detail whilst the experimental observations of Specimen RWT and RWL are briefly described with main focus on how differently these specimens behaved. Fig. 7 displays the lateral load versus top displacement response as well as the maximum out-of-plane displacement at the left boundary region versus top displacement response of Specimen RWB. The sequence of events resulting in the failure of the specimen is indicated in this figure. Fig. 8 displays the crack pattern of Specimen RWB at different drift levels.

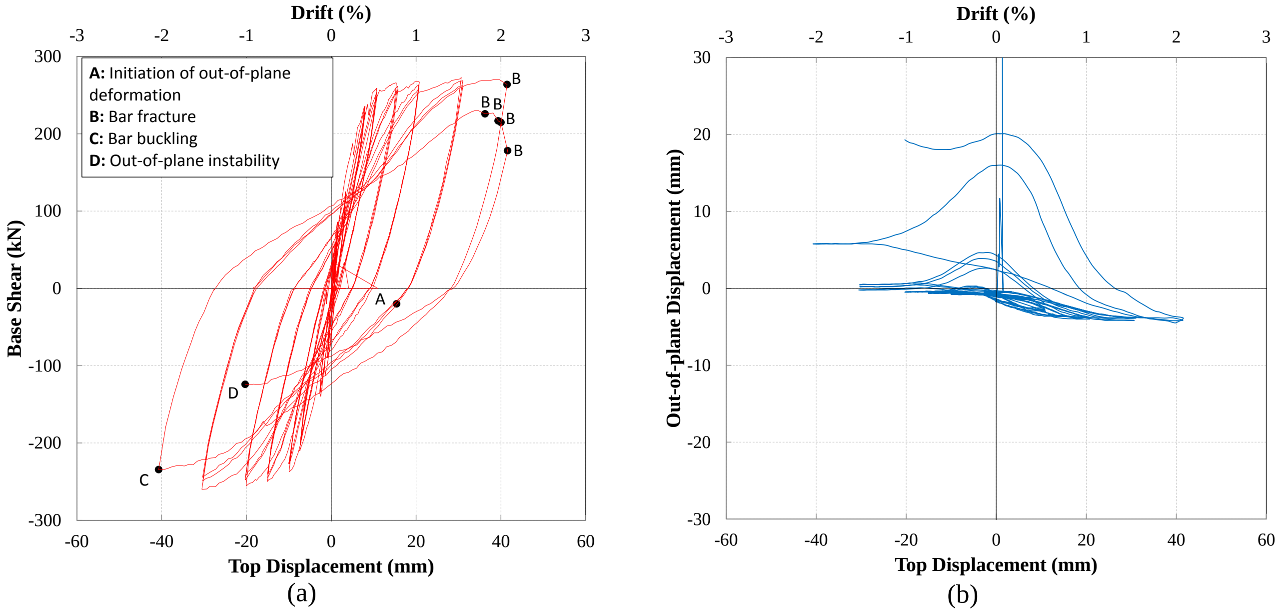

Fig. 7 Experimental response of Specimen RWB: (a) lateral load-top displacement; (b) top displacement vs maximum out-of-plane displacement at left boundary region

Initial cracking happened at 0.05% drift level. As can be seen in Fig. 8, the cracks at this stage are all horizontal flexural cracks mostly located in the boundary zones. At 0.15% drift level, these horizontal cracks extended more with a diagonal orientation at the central region, and more cracks developed up to 1750mm along the height of the specimen. The maximum crack width at this stage was 0.25 mm and the cracks were more distributed in the boundary regions merging into a wider crack in the central panel region. At 0.375% drift level, the cracks increased extensively in terms of number of cracks and length of crack development. The previously formed cracks had a slight increase in crack width. The cracks, with orientations changing from horizontal near the base to vertical along the wall height extended up to 1500mm out of the whole length of 2000mm which shows the considerable movement of the neutral axis position along the wall length. Cracks became wider at 0.5% drift level, especially the diagonal ones, and the ones developed at the base. At this stage, the specimen reached the yield point (Fig. 7a). During 0.75% drift cycle, the cracks did not increase in number and the former cracks became wider and extended up to 1750mm of the wall length. Large crack opening (1.3mm) was observed at the base. During the 3rd cycle of 0.75% drift, cover spalling started on one face of the wall. The cracks became wider during 1.0% and 1.5% drift levels. At 1.5% drift level, the base line crack width was 5.0mm along 500mm from the extreme tension fibre and gradually decreased to 3.0mm and 0.0mm at the 1250 and 1750mm distance from the tension extreme end, respectively. The cracks within 375mm of the wall height had a similar trend. This trend is obviously due to the nonlinear strain profile along the wall length. These cracks were considerably wider when compared to the rest of the wall area. When the specimen was being unloaded and reloaded in the opposite direction, the crack width decreased by about 20-30% when the load reached zero (static residual crack) and by about 50% when the wall displacement reached zero. At this stage, as the load carrying capacity of the wall was provided by the reinforcement that had already undergone a large tensile strain, the specimen started to deform in the out-of-plane direction (Fig. 7b). These wide cracks did not close until about 1.0% drift level in the opposite direction which is the stage when the out-of-plane deformation of the specimen was recovered (Fig. 7b). This phenomenon was repeated in both boundary regions at the subsequent cycles of 1.5% drift level with larger out-of-plane deformations during the second and third cycles as the reinforcement strain increased with the number of cycles.

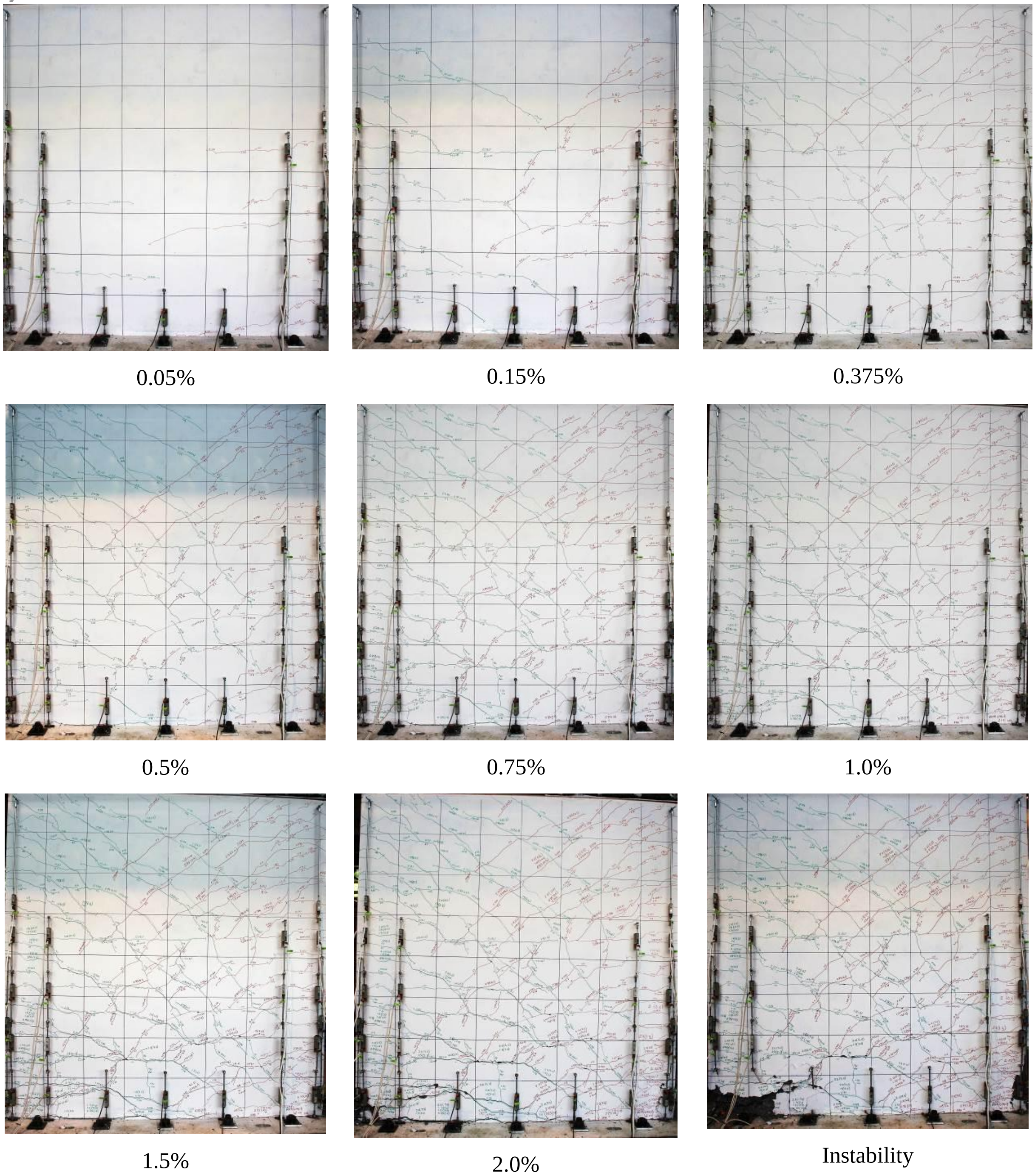

Fig. 8 Crack pattern of Specimen RWB at different drift levels

While reaching the 2.0% drift level, a bar in the extreme tension region snapped. The cracks became wider mostly at the base and within 600mm from the base and the base crack width reached 7.0mm. When the load was applied in the opposite direction, the out-of-plane deformations increased in the left boundary region and reached the maximum value of 17mm at about zero displacement (Fig. 7b). This out-of-plane deformation did not recover completely at the peak displacement of -2.0% drift level and the following cycle started with about 6mm residual out-of-plane deformation in the left boundary zone. At this stage bar buckling was observed at the compression boundary region (Point C, Fig. 7a). During the second cycle of 2.0% drift level, more bar fractures happened at the left boundary region, and the specimen exhibited more out-of-plane deformations when the load was reversed. As can be seen in Fig. 7b, the out-of-plane deformation increased until 0.1% drift level and decreased slightly afterwards but unlike the previous cycle, started to increase. At this stage, an about 50% strength degradation was observed (Fig. 7a) and the test was stopped. Fig. 9 displays some of the observations at ultimate stages of wall response for Specimen RWB.

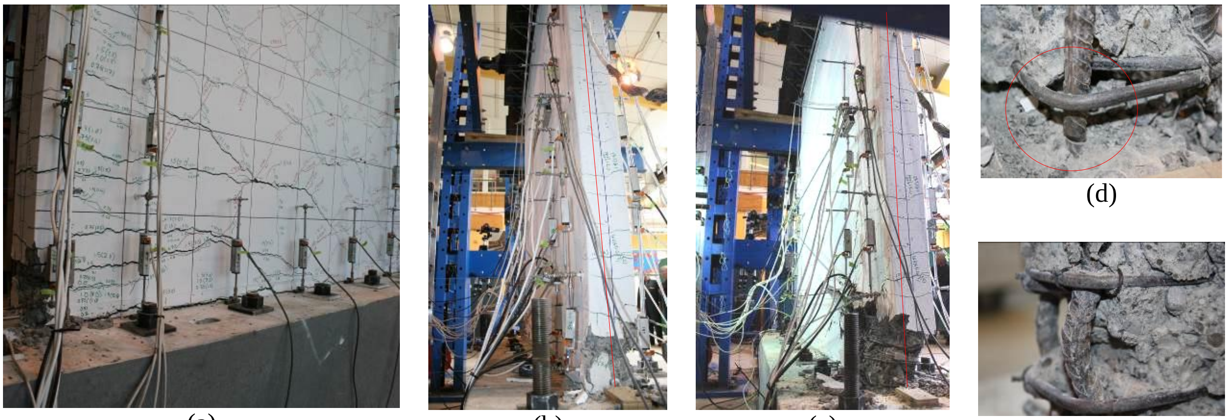

(a) (b) (c) (d) (e)

Fig. 9: (a) Wide cracks, 2.0% drift level; (b) out-of-plane deformation; (c) out-of-plane instability; (d) bar fracture; (e) bar buckling

Fig. 10 displays the test results of Specimens RWT and RWL. Response of Specimen RWT was very similar to the one of Specimen RWB, and its failure initiated with out-of-plane displacements and included bar fracture and bar buckling at later stages of loading. However, the values of out-of-plane displacement were smaller in Specimen RWT when bar fracture had not come into effect which could be due to a slight increase in the wall thickness. The growth of out-of-plane displacement in this specimen as well as its movement from the initial position can be seen in Fig. 10. Specimen RWL was shorter in length and consequently had larger reinforcement ratios in the boundary regions and in the web (Table 1) to provide a flexural capacity close to the other specimens. The failure pattern of this specimen was pure out-of-plane instability with neither bar fracture nor bar buckling being observed during the test. The increasing out-of-plane displacement of the wall did not initially result in a gradual degradation in the lateral load-top displacement response of this specimen, until an abrupt drop of strength occurred after reversing from 3% drift level when the out-of-plane displacement (Fig. 10) did not recover as in the previous cycles and the wall became unstable. The out-of-plane deformation pattern of this specimen is also shown in Fig. 10.

In order to compare the effect of the investigated parameters on out-of-plane deformation of rectangular walls, the out-of-plane deformation of the test specimens is compared at the boundary zones where other failure modes such as bar fracture and bar buckling were not observed. Fig. 11 indicates the out-of-plane displacement profile of the specimens along the wall height in the boundary zones that did not exhibit considerable deterioration due to bar fracture and bar buckling. Since Specimen RWB became unstable during the second cycle of 2.0% drift level, all the out-of-plane displacement profiles are provided up to this level only, for better comparison of the effects of different parameters on this mode of deformation. Although the slight (8%) increase in wall thickness (Specimen RWT as compared to Specimen RWB) did not significantly affect the out-of-plane deformation values at 1.5% drift level, it resulted in about 37% decrease of this type of deformation at 2.0% drift level. Specimen RWL was 20% shorter than Specimen RWB and had a maximum out-of-plane deformation of about 6.7mm during the first cycle of 2.0% drift level which is about 53% reduction compared to 14.1mm out-of-plane deformation of Specimen RWB.

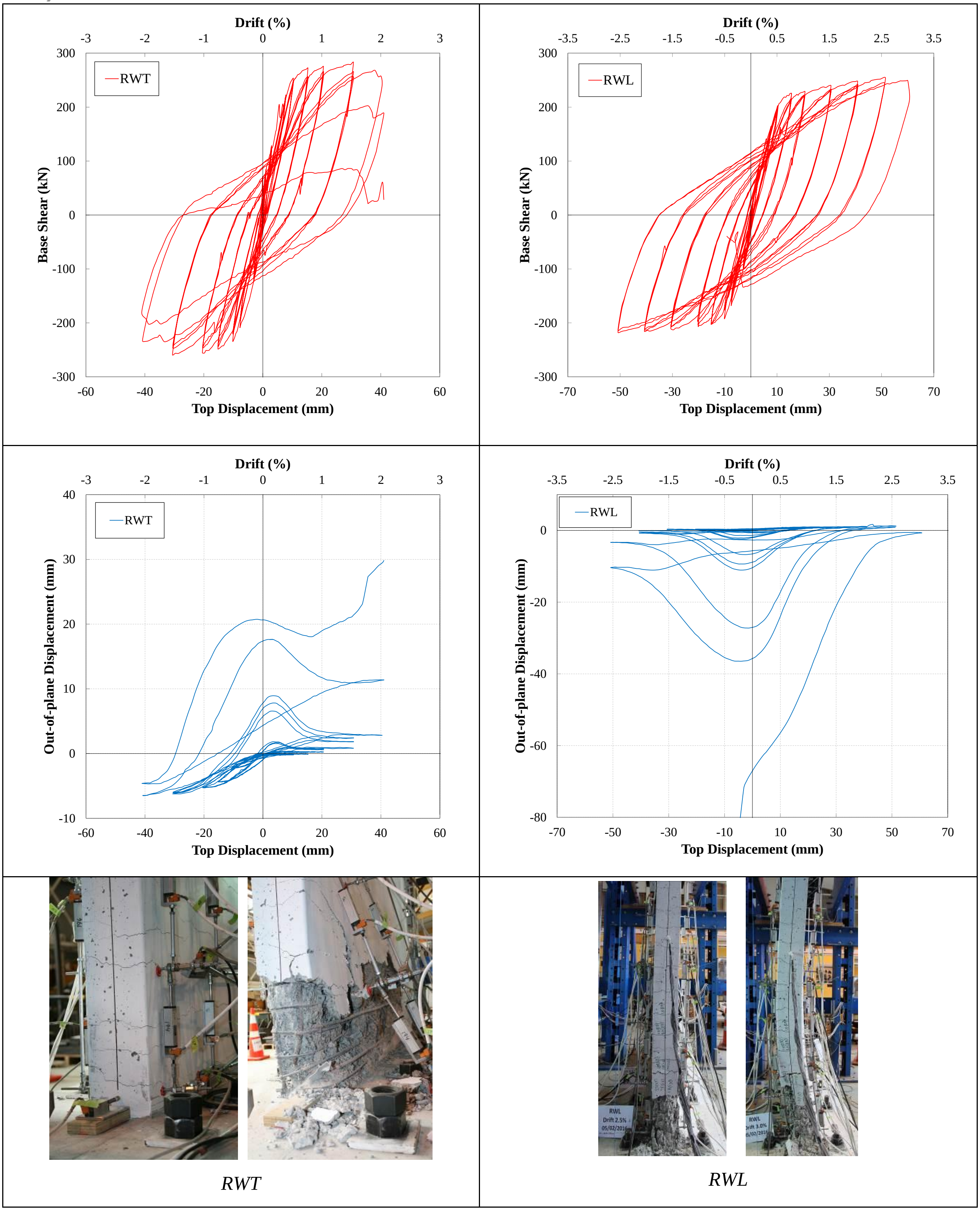

Fig. 10 Experimental response of Specimen RWT and Specimen RWL

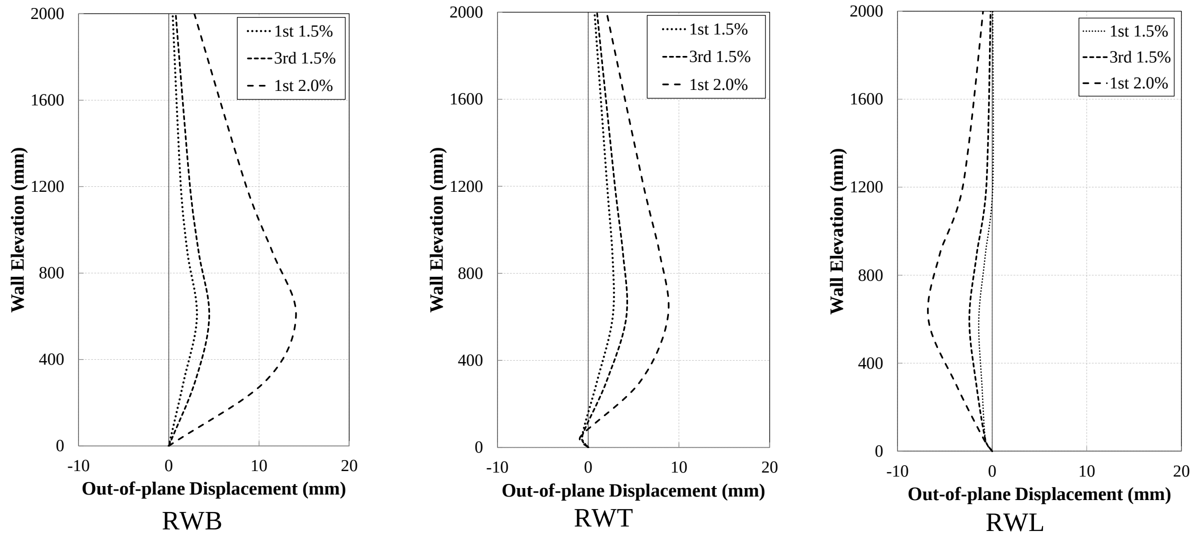

Fig. 11 Out-of-plane displacement profile of the specimens

5. Conclusions

This study investigated, through experimental quasi-static cyclic tests on three half-scaled specimens, the effects of wall thickness and length on the out-of-plane deformation and failure mechanism of rectangular structural walls, designed according to current code provisions.

The slight increase in wall thickness (about 8%) and the 20% reduction in wall length did not change the drift level corresponding to initiation of out-of-plane deformation, but the initial out-of-plane deformation values were slightly less in thicker and shorter walls.

The increase in wall thickness and the reduction in wall length resulted in about 37% and 53% decrease of out-of-plane deformation at 2.0% drift level, respectively.

The failure pattern of the benchmark specimen and the specimen with slight increase in thickness was almost identical, and comprised of out-of-plane deformation initiation at 1.5% drift and bar fracture and bar buckling at 2.0% drift level. Both specimens had strength deteriorations at 2.0% drift level cycles and became unstable with significant movements in the out-of-plane direction at this drift level.

The failure pattern of the shorter specimen was pure out-of-plane instability with neither bar fracture nor bar buckling being observed during the test. This specimen had no strength degradation with increase of out-of-plane deformation until an abrupt drop of strength corresponding to out-of-plane instability at 3.0% drift level.

6. Acknowledgment

The authors wish to acknowledge the financial support provided by the Ministry of Business, Innovation and Employment (MBIE) and the Quake Centre at University of Canterbury to conduct this research.

7. References

[1] Sritharan, S., K. Beyer, R.S. Henry, Y. Chai, M. Kowalsky, and D. Bull (2014): Understanding poor seismic performance of concrete walls and design implications. *Earthquake Spectra*. **30**(1): p. 307-334.
[2] Oesterle, R. (1976): Earthquake Resistant Structural Walls: Tests of Isolated Walls. *Research and Development Construction Technology Laboratories, Portland Cement Association*.
[3] Johnson, B. (2010): Anchorage detailing effects on lateral deformation components of R/C shear walls. *Master Thesis, University of Minnesota*.
[4] Goodsir, W.J. (1985): The design of coupled frame-wall structures for seismic actions. *University of Canterbury*.

[5] Telleen, K., J. Maffei, J. Heintz, and J. Dragovich (2012a): Practical Lessons for Concrete Wall Design, Based on Studies of the 2010 Chile Earthquake. in *15th World Conference on Earthquake Engineering, 24-28 September 2012, Lisbon, Portugal*.
[6] Paulay, T. and M. Priestley (1993): Stability of ductile structural walls. *ACI Structural Journal*. **90**(4).
[7] Chai, Y. and D. Elayer (1999): Lateral stability of reinforced concrete columns under axial reversed cyclic tension and compression. *ACI Structural Journal*. **96**(5).
[8] Rosso, A., J. Almeida, and K. Beyer (2015): Stability of thin reinforced concrete walls under cyclic loads: state-of-the-art and new experimental findings. *Bulletin of Earthquake Engineering*: p. 1-30.
[9] NZS3101 (2006): Concrete Structures Standard, NZS 3101:2006 Parts 1&2 *Standards New Zealand*.
[10] Dashti, F., R. Dhakal, and S. Pampanin (2014a): Numerical simulation of shear wall failure mechanisms. in *2014 NZSEE Conference*. Auckland, New Zealand: New Zealand Society for Earthquake Engineering.
[11] Dashti, F., R. Dhakal, and S. Pampanin (2015): Development of out-of-plane instability in rectangular RC structural walls in *2015 NZSEE Conference*. Rotorua, New Zealand: New Zealand Society for Earthquake Engineering.